Theoretical Study of the Reactivity of Bismuth Oxide Cluster Cations with Ethene in the Presence of Molecular Oxygen

Massimiliano Bienati,[†] Vlasta Bonačić-Koutecký,*[,†] and Piercarlo Fantucci[‡]

Walther-Nernst Institut für Physikalische und Theoretische Chemie, Humboldt-Universität zu Berlin, Bunsenstrasse 1, D-10117 Berlin, Germany, and Dipartimento di Biotecnologie e Bioscienze, P.za della Scienza 1, Università Milano-Bicocca, 20126 Milano, Italy

Received: March 31, 2000

The structural and electronic properties of bismuth oxide clusters of stoichiometry $Bi_3O_y^+$ ($y = 3, 4, 5, 6$) and $Bi_4O_y^+$ ($y = 6, 7, 8$) as well as their interaction with ethene have been investigated using an accurate ab initio density functional approach. The aim of this work is to determine mechanisms under which the metal oxide clusters can invoke transfer of oxygen atoms to unsaturated organic substrates leading to oxygenated compounds. Our findings show that stable bismuth oxide clusters such as $Bi_3O_4^+$ oxidize ethene only in the presence of molecular oxygen. This means that transfer of oxygen atoms from the cluster framework does not occur due to strong Bi−O bonding. We identified the $(Bi_4O_6^+)C_2H_4$ complex with a radical center located at a carbon atom which allows the molecular oxygen to form "superoxide" $(Bi_4O_6^+)C_2H_4-O_2$ species and permits addition of another ethene to form the peroxide $(Bi_4O_6^+)C_2H_4-O_2C_2H_4$. These findings support experimental results of the accompanying paper in this issue. Moreover, we found that an oxirane molecule can be released from the peroxide form, allowing the formation of reactive chain units $(Bi_4O_6^+)-(C_2H_4-O)$ which might be an interesting species for studying the role of bismuth oxide clusters in catalytic processes.

1. Introduction

Bismuth oxides in combination with different transition metal (M) oxides (vanadium, iron, molybdenum[1]) have been widely studied as catalysts in hydrocarbon oxidation processes.[2] Attempts to define a possible reaction mechanism by studying deuterated alkenes forms interacting with ^{17}O-enriched catalysts led to a model based on the assumption that the hydrocarbon oxidation proceeds via the transfer of one oxygen atom bound to the transition metal whereas another oxygen atom bound to bismuth favors the abstraction of hydrogen from the alkenes.[3] According to this model, the activated oxygen could bridge two metal atoms (Bi−O−M)[2] or bind to the transition metal with terminal bond (M = O); in both cases the M center plays a key role in the oxygen transfer reaction. Swift et al.[4] showed that pure solid Bi_2O_3 under suitable reaction conditions could be catalytically active; in addition it was proposed that only terminal oxygen may react with the unsaturated substrate.[5]

Gas phase mass-selected experiments carried out on bismuth oxide clusters by Kinne et al.[6] have evidenced that peaks of stable species deplete in the presence of propene. The experiments have been carried out by scattering a mixture of stable bismuth clusters with general stoichiometry $[BiO^+(Bi_2O_3)_n]$[6−8] in a reaction cell fed with propene at different partial pressures both under canonical and single collision conditions (cf. refs 6−8 for details). By comparing the extent of the depletion of the bismuth oxide mass peaks in the presence of the hydrocarbon with the depletion of the same peaks in the presence of inert gases, a conclusion has been drawn that these clusters should be studied as models for catalysts in oxidation processes of unsaturated hydrocarbons. However, the experimental setup did not allow for a characterization of the reaction products. More recently Fielicke and Rademann. (cf. accompanying paper in this issue[9]) carried out experiments on the same species with the aim to determine the reaction products. They have found that the cluster with stoichiometry $Bi_3O_4^+$ forms stable complexes when interacting with alkenes, but also in this case ethene and propene oxides as neutral products have not been identified. A novel finding of these experiments is that the stable bismuth oxide cluster series with stoichiometry $(Bi_2O_3)_n^+$ ($n \geq 2$) yields particularly high reactive cross sections when interacting with alkenes. Moreover, direct evidence of oxidative properties of these clusters with respect to ethene (and propene) via activation of molecular oxygen has been observed.

Since bismuth oxide clusters might serve as model systems for oxidation catalysts, we carried out first a systematic theoretical study of the ground state properties of the stoichiometric $Bi_3O_4^+$ and $Bi_4O_6^+$ species and their oxygenated forms. In addition, their chemical behavior in the presence of ethene and molecular oxygen has been investigated by following different reaction paths including: (i) direct oxygen transfer reactions from the cluster to the alkene π bond, (ii) formation of stable intermediates between the clusters and the unsaturated hydrocarbons, (iii) activation of molecular oxygen by the cluster and oxygen transfer reactions to the alkenes; (iv) chain reactions of radical species supported on the cluster subunit.

The aim of the present work is to gain a better understanding of the general chemical behavior of oxygenated Bi clusters by the identification and energetic characterization of the different chemical species involved in the reactive process.

The paper is organized as follows: after outlining the computational procedures in section 2, we present the results of ground state properties of bismuth oxide clusters (section 3). We address the role of $Bi_3O_y^+$ ($y = 4, 5, 6$) and $Bi_4O_y^+$ ($y = 6, 7, 8$) clusters in the oxidation of π bonds in sections 4 and 5, respectively. Important properties of $Bi_4O_6^+$ species as a possible model system to study catalytic processes are presented in section 6, while conclusions with outlook are given in Section 7.

[†] Humboldt-Universität zu Berlin.
[‡] Universitá Milano-Bicocca.

10.1021/jp001258e CCC: $19.00
Published on Web 07/07/2000

TABLE 1: Comparison of Calculated and Experimental[a] Properties of Bi Atom, Bi_2, BiO and BiO^+ Dimers

	IP (eV)	EA (eV)
Bi		
this work	7.580	0.557
expt[a]	7.285	0.910
	R_0 (Å)	D_0 (kcal mol^{-1})
Bi_2		
this work	2.906	48.00
expt[a]		47.89
BiO		
this work	1.905	79.90
expt[a]	1.934	80.55
BiO^+		
this work	1.792	100.21

[a] Experimental data for ionization potential (IP), electron affinity (EA), bond distances, and dissociation enthalpies D_0 at 298 K from ref 16.

2. Computational Methods

All the ground state (GS) structural properties of the oxide clusters as well as the structures of the transition states (TS) along the different investigated reaction paths have been computed with spin-polarized density functional theory (DFT) based on the non local exchange and correlation functionals proposed by Becke[10] (B97). The reliability of these new functionals has been tested on the G2 thermochemical data set,[11] and an improvement with respect to the commonly used hybrid three-parameter B3LYP functional[12] has been achieved for calculation of atomization energies and molecular geometries[13] as well as vibrational frequencies.[14] To reduce the computational effort, the effects of the core electrons have been represented by the effective core potential (ECP) proposed by Krauss et al.[15] for Bi atom and by Basch et al.[16] for oxygen and carbon atoms. For the valence orbitals of the Bi atom the double-ζ ECP-AO basis set of ref 15 augmented by a d polarization function with exponent 0.200 has been used. For oxygen and carbon atoms, we adopted the associated basis set of ref 16 of double-ζ type which has been augmented by sp diffuse functions (with exponents 0.0438 and 0.0845, respectively) and by a d polarization function (with exponents 0.750 and 0.800, respectively). The computed ground state properties of Bi_2, BiO^+, and BiO are in excellent agreement with experimental data[17] as shown in Table 1, giving us the confidence about the accuracy of chosen functionals, ECPs and AO basis set.

Critical points on the Born−Oppenheimer potential energy surface (PES) (cf. ref 18 and references therein) associated with stable reactants, intermediates, and products have been determined by gradient-based energy minimization methods (cf. ref 19 and references therein) using the Gaussian 98 quantum chemistry package.[21] Transition state (TS) structures have been obtained using the synchronous transit guided quasi-Newton (STQN) method developed by Schlegel and co-worker[20] as implemented in the Gaussian 98[21] code.

The relative stability of the computed cluster structures is discussed in terms of binding energy (BE) per atom defined as

$$\mathrm{BE}/(x+y) = \frac{E(\mathrm{Bi}_x\mathrm{O}_y^+) - E(\mathrm{Bi}^+) - (x-1)E(\mathrm{Bi}) - yE(\mathrm{O})}{x+y}$$

At each critical point on the PES (obtained with the convergence criteria 10^{-4} for gradients) analytical forces have been computed and vibrational frequency analysis has been carried out. These quantities have been used in addition to the total energy of the system to obtain the thermodynamic properties (cf. for example ref 22) of the investigated species

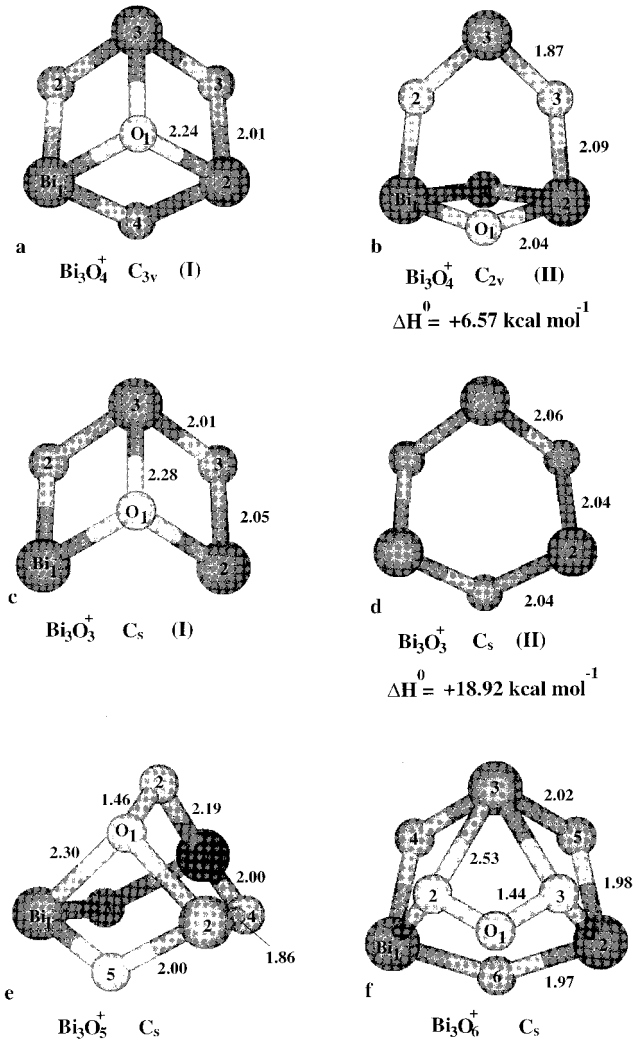

Figure 1. The most stable structures with symmetry labels of the $Bi_3O_y^+$ ($y = 3-6$) clusters (isomers I) obtained from DFT approach of section 2. For the $Bi_3O_4^+$ and $Bi_3O_3^+$ isomers II (with symmetry labels) are also displayed with the corresponding enthalpy differences $\Delta H°$ in kcal mol^{-1} (cf. Table 2). Bond lengths are given in angstroms in all figures.

in order to describe the chemical processes in terms of a canonical ensemble of interacting particles in the framework of the generalized transition state theory (GTST) (cf. ref 23 and references therein). All reactions have been considered as bimolecular reactions, and no tunneling effects as well as vibrational anharmonicities have been taken into account. The TS structures have been optimized by imposing severe convergence criteria (10^{-8} for the electronic density), and the influence of the coupling of the real vibrational normal modes of the TS complex to the imaginary reaction path mode (which is treated classically in the GTST) has been avoided by the projection technique proposed by Baboul and Schlegel.[24] To avoid artificial distortions of the PES it was carefully checked that the spin contamination of the wave function (density matrix) inherent to the UHF/KS method remains low also during breaking of chemical bonds. Charge population analysis based on the natural atomic orbital (NAO) scheme (cf. ref 25 and references therein) has been preferred to the classical Mulliken scheme[26] due to several recognized deficiencies of the latter.[27]

3. Structures and Energetics of the Bismuth Oxide Clusters. According to experimental findings[6−8] $Bi_3O_4^+$ and $Bi_4O_6^+$ (cf. accompanying paper[9]) clusters play an important role in reactions with alkenes. Therefore we first address ground

TABLE 2: Ground State Energies and Properties of $Bi_3O_y^+$ ($y = 3, 4, 5, 6$) and $Bi_4O_y^+$ ($y = 6,7$) Clusters

cluster[a]	sym	E_{DFT} (au)	$H°_{DFT}$[b] (au)	$\Delta H°$[c] (kcal mol^{-1})	BE/$(x+y)$[d] (kcal mol^{-1})
$Bi_3O_4^+$ (I)	C_{3v}	−79.823 589	−79.802 654		86.56
$Bi_3O_4^+$ (II)	C_{2v}	−79.813 062	−79.792 179	6.57	85.61
$Bi_3O_3^+$ (I)	C_s	−63.790 459	−63.773 254		78.28
$Bi_3O_3^+$ (II)	C_s	−63.760 060	−63.743 084	18.92	75.10
$Bi_3O_5^+$ (I)	C_s	−95.728 845	−95.703 750		82.73
$Bi_3O_6^+$ (I)	C_s	−111.624 036	−111.594 488		79.05
$Bi_4O_6^+$ (I)	C_s	−117.166 494	−117.135 976		86.94
$Bi_4O_6^+$ (II)	C_s	−117.117 387	−117.086 719	30.91	83.86
$Bi_4O_6^+$ (III)	C_s	−117.087 749	−117.056 473	49.89	82.00
$Bi_4O_6^+$ (IV)	C_{2v}	−117.047 366	−117.015 687	75.48	79.47
$Bi_4O_7^+$ (I)	C_s	−133.074 809	−133.040 041		84.30
$Bi_4O_7^+$ (II)	C_s	−132.946 195	−132.912 880	79.80	76.96

[a] For geometries of clusters cf. Figure 1 and 2; I to IV label isomers according to the energy ordering. [b] The $H°_{DFT}$ is the sum of DFT electronic energy and thermal correction to enthalpy at 298 K. [c] The DFT enthalpy difference between isomers. [d] Binding energy per atom (cf. section 2). (E(Bi) = −5.29076213917 au; E(Bi$^+$) = −5.01218221603 au; E(O) = −15.8160885040 au).

TABLE 3: NAO Charge Population Analysis of the Most Stable Structures of $Bi_3O_y^+$ ($y = 3, 4, 5, 6$) and $Bi_4O_6^+$ Clusters

atoms	$Bi_3O_4^+$ [a]	$Bi_3O_3^+$ [a]	$Bi_3O_5^+$ [a]	$Bi_3O_6^+$ [a]	$Bi_4O_6^+$ [b]
O_1	−1.44	−1.40	−0.75	−0.07	−1.42
Bi_1	2.19	1.47	2.20	2.21	2.23
O_2	−1.38	−1.35	−0.63	−0.68	−1.42
Bi_2	2.19	1.47	2.20	2.21	2.21
O_3	−1.38	−1.35	−1.40	−0.68	−1.43
Bi_3	2.19	2.18	2.17	2.21	2.21
O_4	−1.38		−1.40	−1.39	−1.42
O_5			−1.39	−1.39	−1.42
Bi_4				-	2.23
O_6				−1.43	−0.76

[a,b] For structures and atom labels of the cluster cf. Figure 1 and Figure 2, respectively.

state properties of these clusters and their derivatives in the context of the role they might play in oxidation processes of unsaturated hydrocarbons.

3.1. The $Bi_3O_4^+$ Cluster and Its Derivatives. The ground state of $Bi_3O_4^+$ assumes a closed shell electronic configuration. The computed most stable structure with C_{3v} symmetry shown in Figure 1a has been also previously reported.[6−8] The second isomer with the C_{2v} symmetry (Figure 1b) lies relatively close in energy to the C_{3v} structure. The enthalpy difference between the two isomers computed at 298 K is 6.6 kcal mol^{-1} with an isomerization barrier of 7.6 kcal mol^{-1}, indicating their possible coexistence at room temperature. A Bi−O−Bi binding subunit with an average Bi−O distance of 2.08 Å characterizes both isomers, but in the C_{3v} isomer (1a) the μ_3 (capping) oxygen has longer distance (2.25 Å) than the μ_2 (bridging) oxygens in the C_{2v} isomer (1.94 Å) (1b). These values compare well with the bond distances in the BiO and BiO$^+$ dimers (see Table 1). Further analysis of geometrical data yields an average O−O distance of 2.80 Å, revealing a pronounced compactness of these species and the absence of dioxygen bonds. The binding energies per atoms given in Table 2 also compare well with the corresponding BiO and BiO$^+$ dissociation energies reported in Table 1, reflecting a very high cluster stability due to the absence of metal−metal bonds and to the presence of very stable Bi−O covalent bonds. Furthermore, according to NAO charge population analysis (Table 3) the average partial charge of Bi atom is ∼2.2 charge units which differs substantially from the formal oxidation state (+3) in ionic compounds, emphasizing the covalent character of the Bi−O bonds in clusters. Other isomers with terminally bound oxygen or with higher multiplicity have considerably higher energies with respect to the isomers in Figure 1a,b (cf. ref 6a) and have not been considered further in the present study.

The removal of the μ_3 oxygen from the isomer in Figure 1a of the $Bi_3O_4^+$ cluster gives rise to the $Bi_3O_3^+$ species (Figure 1c) with singlet ground state. The second isomer of $Bi_3O_3^+$ (Figure 1d) with the ring structure has considerably higher enthalpy (18.92 kcal mol^{-1}). The calculated BE per atom of the stable $Bi_3O_3^+$ structure is 78.3 kcal mol^{-1} (Table 2). However, this cluster can be considered as unstable toward oxidation, since an energy of +136.1 kcal mol^{-1} is needed for the extraction of one of the oxygens from the $Bi_3O_4^+$ cluster, whereas the $Bi_3O_3^+$ oxidation by molecular oxygen results in an extremely exoergic process (−72.7 kcal mol^{-1}) since the reaction energy barrier has not been located.

The structure of the oxygenated cluster of stoichiometry $Bi_3O_5^+$ shown in Figure 1e exhibits very interesting properties. In fact, some reactions on metal oxides investigated in connection with oxidation catalysts are induced also by dioxygen species.[28,29] The computed structure of this cluster has a molecular subunit similar to the $Bi_3O_4^+$ C_{2v} cluster with an additional oxygen bound to a metal atom and to another oxygen atom with distances 2.02 and 1.46 Å, respectively. By comparing the dioxygen bond length in the cluster with the experimental value of the free molecular oxygen in its electronic ground state ^{3}P (1.21 Å)[17] and with the computed bond distance of the O_2^{2-} peroxide adsorbed on metals (1.49 Å),[28,29] the conclusion can be drawn that this cluster strongly supports an activated dioxygen species. In fact, the computed vibrational frequency of 928.4 cm^{-1} associated with the stretching of the O_2 group in the $Bi_3O_5^+$ cluster compares well to the experimental ν(O−O) vibrational energy (700−900 cm^{-1}) of peroxide groups on different metal complexes.[28] However, the NAO charge distribution analysis of Table 3 shows that the excess of negative charge on the dioxygen group is smaller (−1.38 charge units) than in the free peroxo anion. This confirms that the elongation of the O−O distance in the bismuth oxide is not necessarily caused by a large negative charge on the dioxygen group itself, and therefore its classification as peroxide should be considered as very approximate.

The ground state structure of the $Bi_3O_6^+$ cluster contains an ozonide-like group (cf. Figure 1f), and according to thermochemical analysis it can be considered as a thermodynamically unstable compound exhibiting only kinetic stability (cf. Table 2). $Bi_3O_6^+$ can be produced by direct oxidation of $Bi_3O_4^+$ with a reaction enthalpy of +11.4 kcal mol^{-1} and an activation barrier of +32.9 kcal mol^{-1}. The key role of this compound will be pointed out in connection with the role of bismuth oxide clusters in alkene oxidation processes.

3.2. The $Bi_4O_6^+$ Cluster and Its Derivatives. The computed most stable structure of the $Bi_4O_6^+$ cluster with C_s symmetry arises from the Jahn−Teller distortion of the most symmetric C_{3v} structure as shown in Figure 2a. It exhibits a pronounced compact molecular skeleton, which maximizes the number of Bi−O bonds avoiding any Bi−Bi and O−O bonds. Notice that this structure closely resembles the well-known P_4O_6 and As_4O_6 species. The second isomer with compact structure as well as other two isomers containing O−O bonds and terminal oxygen atoms are shown in Figure 2b−d. They lie more than 30.0 kcal mol^{-1} higher in energy with respect to the isomer in Figure 2a (cf. Table 2) and have not been considered further as important species in the present study. In the isomer I of $Bi_4O_6^+$ (Figure 2a) the unpaired electron is localized on the mostly exposed bridging oxygen atom. The corresponding electronic configuration gives rise to the pronounced charge distribution on this

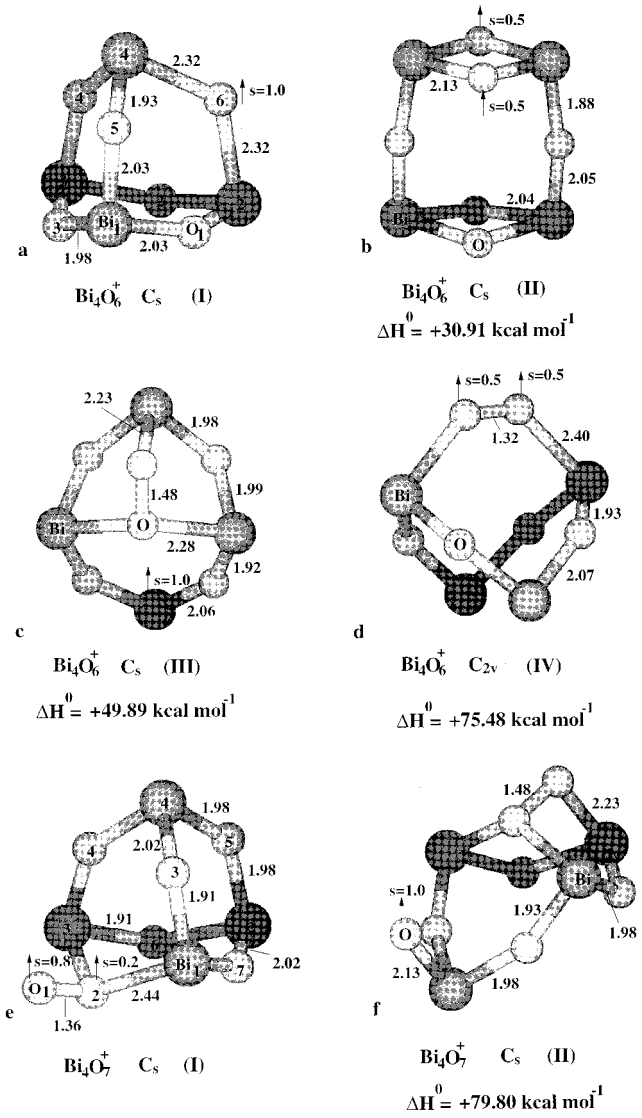

Figure 2. The most stable structures of $Bi_3O_y^+$ ($y = 6, 7$) (isomers I) as well as isomeric forms with higher energies, with symmetry labels and corresponding enthalpy differences $\Delta H°$ in kcal mol^{-1} obtained from DFT approach (cf. section 2). Spin population of the unpaired electron has been assigned to the corresponding atom.

atom as reported in Table 3, which allows us to consider the cluster as a radical species.

The most stable structure of the $Bi_4O_7^+$ cluster shown in Figure 2e contains a dioxygen form, and the unpaired electron is shared by both oxygen atoms with different weights. Similarly, as in the case of $Bi_4O_6^+$, the second isomer of $Bi_4O_7^+$ lies more than 30.0 kcal mol^{-1} higher in energy with respect to the most stable one (cf. Figure 2f and Table 2) and therefore will be not further considered.

Highly oxygenated cluster forms, such as $Bi_4O_8^+$ species, are not stable, being characterized by a positive formation enthalpy in agreement with the experimental findings (cf. accompanying paper[9]).

4. The Role of $Bi_3O_y^+$ ($y = 4, 5, 6$) Clusters in the Oxidation of π Bonds

In this section we wish to address the oxidative properties of the $Bi_3O_y^+$ ($y = 4-6$) series with respect to π bonds in alkenes. We have chosen to present results with ethene in the present paper since we have found that other nonconjugated unsaturated hydrocarbons (such as propene) do not influence significantly the energetics of the investigated reactions. Reaction channels for the oxygen transfer have been intuitively selected. However, the TS structures have been located without any constraints to geometrical parameters and molecular symmetry. The results on energetics are summarized in Table 4.

TABLE 4: Ground and Transition State (TS) Energies of $Bi_3O_y^+$ ($y = 4, 5, 6$) Clusters Interacting with Ethylene

structures	E_{DFT} (au)	$H°_{DFT}$ (au)
$(Bi_3O_4^+)C_2H_4$ (I)[a]	−93.506 793	−93.428 894
$(Bi_3O_4^+)C_2H_4$ (II)[a]	−93.486 241	−93.408 694
$(Bi_3O_4^+)C_2H_4$ (TS)[a]	−93.475 263	−93.398 676
$(Bi_3O_4^+)C_2H_4$ (TS)[b]	−93.385 643	−93.308 132
$(Bi_3O_5^+)C_2H_4$ (TS)[c]	−109.366 668	−109.286 238
$(Bi_3O_6^+)C_2H_4$ (TS)[d]	−125.247 975	−125.163 216
O_2[e]	−31.8170 39	−31.809 969
C_2H_4[f]	−13.656 457	−13.601 838
OC_2H_4[g]	−29.608 472	−29.547 570

[a] For geometries of clusters cf. Figure 4; I and II label isomers according to the energy ordering; TS labels the structure of the activated complex for the formation of the most stable isomer I. [b−d] For the geometry of the activated complex, cf. Figure 3, Figure 5, and Figure 6, respectively. [e−g] Energies and enthalpies for stable structures of molecular oxygen, ethene, and oxirane, respectively.

4.1. $Bi_3O_4^+$ and C_2H_4. The oxygen transfer reaction from the stoichiometric $Bi_3O_4^+$ cluster (in both C_{3v} and C_{2v} isomeric forms) to ethene and involving oxirane as oxidized product[30] is an unfavorable process from both thermodynamic and kinetic points of view (cf. Table 4). The enthalpy for the reaction

$$Bi_3O_4^+ + C_2H_4 \rightarrow Bi_3O_3^+ + OC_2H_4$$

calculated at 298 K and involving isomer I (Figure 1a) of $Bi_3O_4^+$ is +52.5 kcal mol^{-1} with an activation barrier of +60.5 kcal mol^{-1}. This is mainly due to the fact that the process involves the breaking of a strong Bi−O bond and that the reduced $Bi_3O_3^+$ cluster has lower stability than its oxygenated homologue as has been pointed out in section 3.1. The same oxidation process involving the second isomer II (Figure 1b) of $Bi_3O_4^+$ yields a reaction enthalpy of +45.9 kcal mol^{-1} with an activation barrier of +53.89 kcal mol^{-1} (the lower barrier in the latter case is due to the energy difference between the two isomers). Starting the reaction path from both isomers, the same TS structure shown in Figure 3 has been located implying the involvement of the isomerization of the $Bi_3O_4^+$ clusters in the oxygen transfer process. The NAO charge population analysis of the TS structure reported in Table 5 compared with the values of the free clusters of Table 3 evidences that a strong charge rearrangement occurs both at atoms belonging to the cluster and at carbon atoms of ethene.

The $Bi_3O_4^+$ cluster interacts with ethene by forming stable complexes as shown in Figure 4a,b, probably due to the fact that the positive charge is mostly localized on the metal centers associating the cluster with a Lewis acid. In both isomers of Figure 4, the π character of the carbon−carbon bond is lost and one of the cluster oxygens forms an alcohol-like bond whereas the metal atom acts as acid site. The energy difference between the two isomers (cf. Figure 4a and Figure 4b) is +12.7 kcal mol^{-1} with an isomerization barrier of +13.7 kcal mol^{-1} due to the breaking of a strong Bi−O bond. Notice that the structural subunit of the "pseudo" ethyl alcohol in the framework of the isomer II in Figure 4b is closer associated to the most stable conformation of the free alcohol than in the case of the isomer I Figure 4a. The TS structure for the formation of the isomer I is shown in Figure 4c. The reaction is exoergic by 16.5 kcal mol^{-1}, and the energy barrier has been computed as +3.7 kcal mol^{-1} (cf. Table 4). Furthermore, the values of NAO

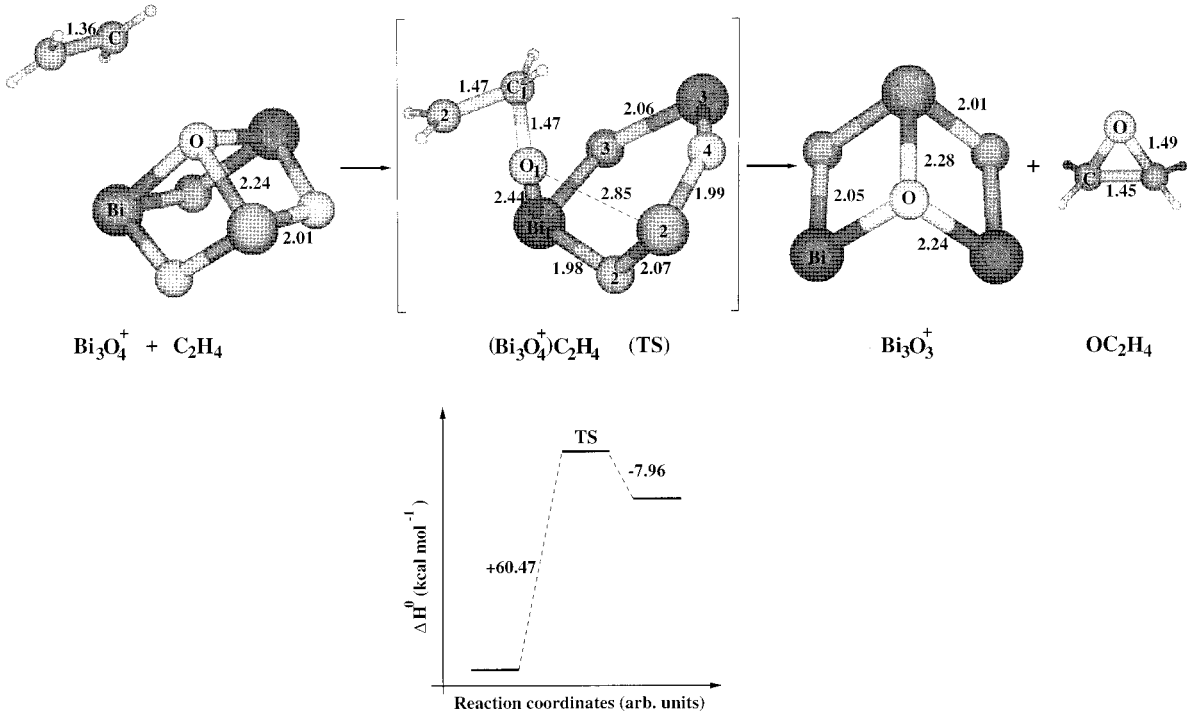

Figure 3. Structures of reactants, TS, and products as well as the energetics for the reaction $Bi_3O_4^+ + C_2H_4 \rightarrow Bi_3O_3^+ + OC_2H_4$ obtained from DFT approach of section 2 (cf. also Table 4).

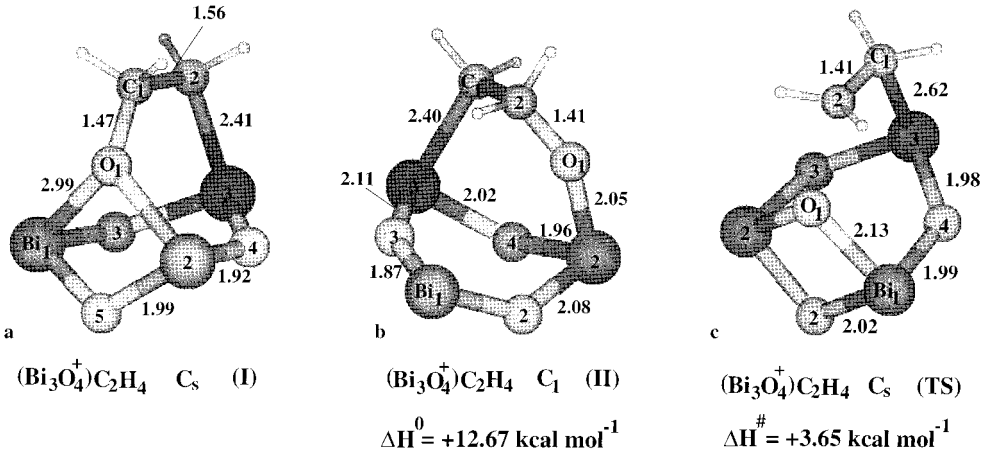

Figure 4. Structures of isomers I and II of $(Bi_3O_4^+)C_2H_4$ complex together with the TS and the corresponding enthalpy differences $\Delta H°$ in kcal mol^{-1} obtained with DFT approach of section 2 (cf. also Table 4).

TABLE 5: NAO Charge Population Analysis of the Transition State Structures of $Bi_3O_y^+$ ($y = 4-6$) Clusters Interacting with Ethylene

	$(Bi_3O_4^+)C_2H_4$ (TS)[a]			$(Bi_3O_5^+)C_2H_4$	$(Bi_3O_6^+)C_2H_4$
atom	I[a]	TS[a]	TS[b]	(TS)[c]	(TS)[d]
O_1	−1.01	−1.34	−0.84	−0.96	−0.32
Bi_1	2.21	2.19	2.12	2.20	2.20
O_2	−1.38	−1.37	−1.39	−0.68	−0.68
Bi_2	2.21	2.19	1.74	2.20	2.21
O_3	−1.40	−1.41	−1.40	−1.38	−0.69
Bi_3	2.02	2.14	1.54	2.20	2.22
O_4	−1.40	−1.41	−1.38	−1.41	−1.39
O_5				−1.41	−1.39
O_6				-	−1.39
C_1	−0.98	−0.85	−0.12	−0.18	−0.25
C_2	−0.08	−0.11	−0.18	−0.52	−0.40

[a–d] For structures and atom labels of the cluster cf. Figure 4, Figure 3, Figure 5, and Figure 6, respectively.

charge population analysis for isomers in Figure 4a,b and for the TS of $(Bi_3O_4^+)C_2H_4$ reported in Table 5 evidence that the hydrocarbon loses its π character already in the activated complex.

4.2. $Bi_3O_y^+$ ($y = 5$, 6) and C_2H_4. The ethene oxidation reaction involving the $Bi_3O_5^+$ cluster is thermodynamically favorable and the relatively low reaction energy barrier offers also accessible kinetics as expected from the results of section 3.1. In fact, the reaction enthalpy of the process

$$Bi_3O_5^+ + C_2H_4 \rightarrow Bi_3O_4^+ + OC_2H_4$$

amounts to −28.0 kcal mol^{-1} with an activation barrier of +12.1 kcal mol^{-1} (cf. Figure 5 and Table 4). The reactive interaction gives rise to more pronounced charge redistributions on both carbon atoms than in the other cases (cf. Table 5). Furthermore, the TS structure closely resembles the geometry of reactants, in agreement with the prediction of the Hammond's postulate for exoergic reactions.

According to results of section 3.1, the $Bi_3O_6^+$ oxide is thermodynamically unstable but kinetically stable; analogous behavior of the free O_3 suggested us to investigate the thermochemistry of the following reaction:

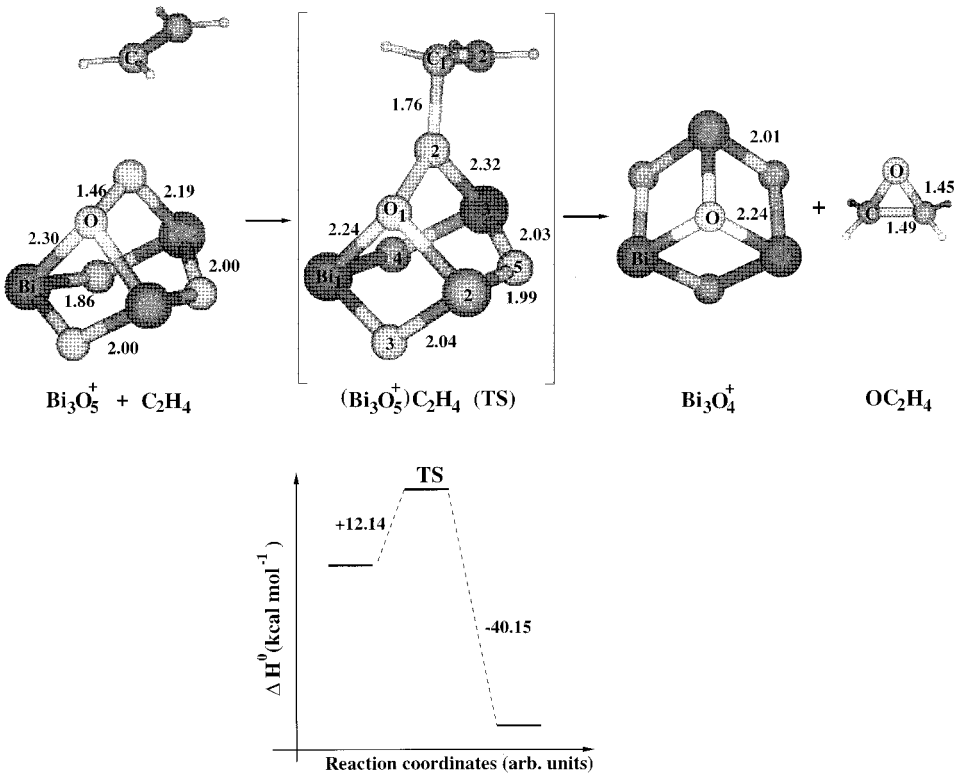

Figure 5. Structures of reactants, TS, and products as well as the energetics for the reaction $Bi_3O_5^+ + C_2H_4 \rightarrow Bi_3O_4^+ + OC_2H_4$ obtained from DFT approach of section 2 (cf. also Table 4).

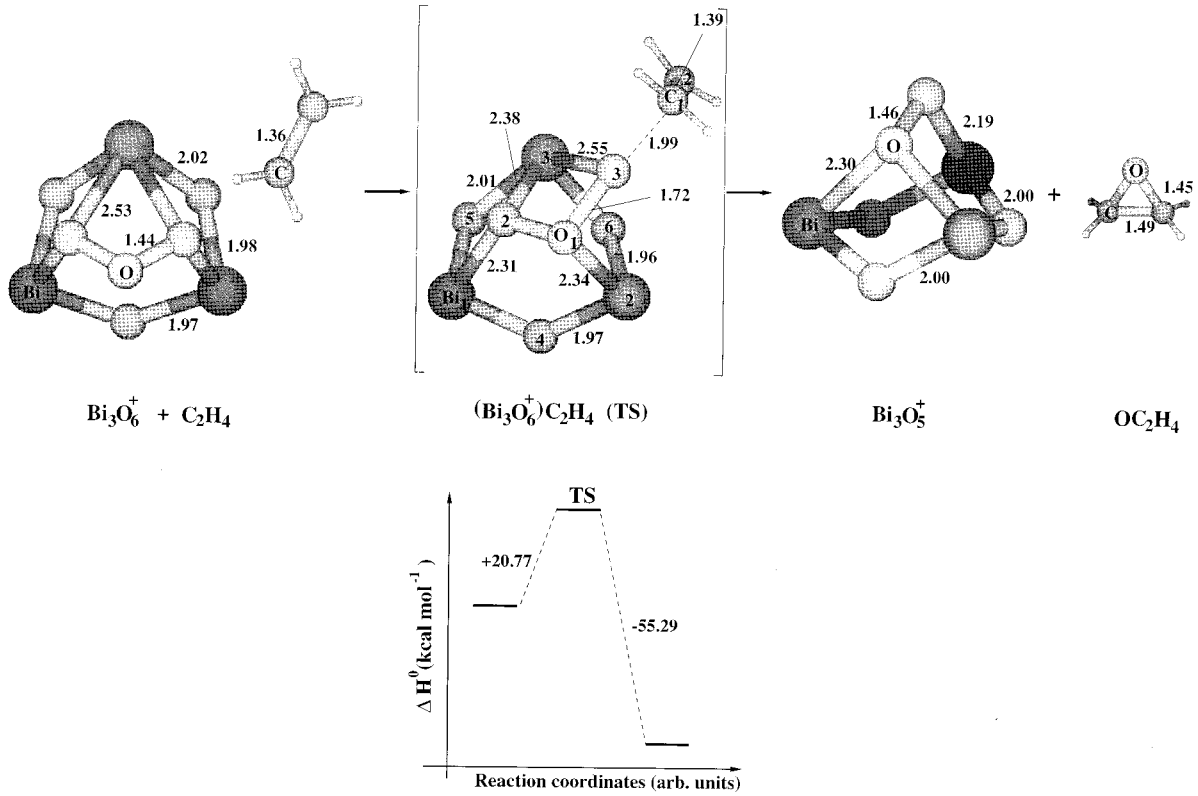

Figure 6. Structures of reactants, TS, and products as well as the energetics for the reaction $Bi_3O_6^+ + C_2H_4 \rightarrow Bi_3O_5^+ + OC_2H_4$ obtained from DFT approach of section 2 (cf. also Table 4).

$$Bi_3O_6^+ + C_2H_4 \rightarrow Bi_3O_5^+ + OC_2H_4$$

This reaction is exoergic by 34.5 kcal mol^{-1} and has to overcome a barrier of +20.8 kcal mol^{-1} in order to take place (cf. Figure 6 and Table 4). This result is important for determining the role of $Bi_3O_4^+$ cluster in the first step oxidation[30] of organic π species as will be discussed in the next section.

4.3. The Role of Molecular Oxygen in the Presence of Stable Clusters in the Oxidation of π Bonds. As mentioned

in the Introduction, Kinne et al.[6] proposed that the $Bi_3O_4^+$ cluster can be used as a model system to study catalytic properties of bismuth oxides in oxidation processes of alkenes. The global gas phase oxidation reaction of ethene (or π bonds in general) involving the $Bi_3O_4^+$ species proceeds according to the following chemical equation to form oxirane:[30]

$$Bi_3O_4^+ + 2C_2H_4 + O_2 \rightarrow Bi_3O_4^+ + 2OC_2H_4$$

with a reaction enthalpy of $\Delta H°_{298} = -51.1$ kcal mol $^{-1}$ which is a thermodynamically favorable process.

To obtain an oxidative catalytic cycle involving transfer of oxygen from the $Bi_3O_4^+$ cluster to the alkenes, a large amount of energy is needed to overcome the activation barrier leading to the oxidized hydrocarbon as demonstrated in section 4.1. This shows that the cluster alone cannot act as catalyst by transferring its own oxygen atoms. On the other hand, the oxidation of ethene by $Bi_3O_5^+$ shows a favorable thermodynamics and kinetics as pointed out in section 4.2. Moreover, once the $Bi_3O_6^+$ has been formed it reacts easily further to form oxirane and $Bi_3O_5^+$ as products.

On the basis of the above results, we propose a three-step oxidation process according to the global thermodynamic cycle shown in Figure 7 (cf. also Tables 3 and 4).

first step:

$$Bi_3O_4^+ + O_2 \rightarrow Bi_3O_6^+$$

$\Delta^1H°_{298} = +11.4$ kcal mol^{-1}; $\Delta^1H^{\#}_{298} = +32.9$ kcal mol^{-1}

second step:

$$Bi_3O_6^+ + C_2H_4 \rightarrow Bi_3O_5^+ + OC_2H_4$$

$\Delta^2H°_{298} = -35.4$ kcal mol^{-1}; $\Delta^2H^{\#}_{298} = +20.8$ kcal mol^{-1}

third step:

$$Bi_3O_5^+ + C_2H_4 \rightarrow Bi_3O_4^+ + OC_2H_4$$

$\Delta^3H°_{298} = -28.0$ kcal mol^{-1}; $\Delta^3H^{\#}_{298} = +12.1$ kcal mol^{-1}

The thermodynamic energy balance gives rise to $\Delta^1H°_{298} + \Delta^2H°_{298} + \Delta^3H°_{298} = -51.1$ kcal mol^{-1} corresponding to the energetics of the stoichiometric reaction $2C_2H_4 + O_2 \rightarrow 2OC_2H_4$. Furthermore, the high exoergicity of the second and third steps compared to the activation enthalpy at each step suggests that once the first reaction has been activated the cycle will self-propagate. However, according to our findings (cf. Section 4.1) which have been confirmed also by the experimental results reported in the accompanying paper,[9] the $Bi_3O_4^+$ cluster interacting with π systems has a strong tendency to form stable complexes. This makes the discussed cycle, which in principle can exist, very difficult to be realized.

The important finding of this section is that the presence of molecular oxygen is necessary to provoke the reactivity of the cluster, which initiated further experimental as well as theoretical work which we present in the next section.

5. The Role of $Bi_4O_y^+$ ($y = 6, 7, 8$) Clusters in the Oxidation of π Bonds

The most stable structure of the $Bi_4O_6^+$ cluster has been characterized as a radical species in section 3.2. According to

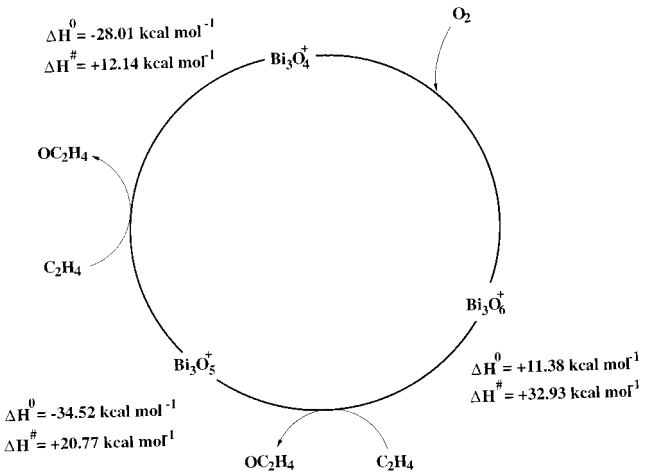

Figure 7. Energetics of the thermodynamic cycle starting from $Bi_3O_4^+$ in the presence of molecular oxygen and ethene to form oxirane.

experimental observation (cf. accompanying paper[9]) this species exhibits particularly large reactive cross sections when interacting with a mixture of alkene and molecular oxygen, leading to the formation of compounds with identified masses corresponding to stoichiometry $Bi_4O_8^+(C_2H_4)_z$ ($z = 1, 2$). However, from both experimental evidence and theoretical prediction the free species $Bi_4O_8^+$ is expected to be unstable. This fact suggested to us to investigate the gas phase reactivity of the $Bi_4O_6^+$ cluster in stepwise reactions involving ethene as first reactant. The results are summarized in Figure 8 and Table 6, which will be used for further discussion.

There is evidence that the bismuth oxide clusters can easily bind one or more ethene molecules (cf. accompanying paper[9]). This is also the case of the $Bi_4O_6^+$ species, which forms a stable complex $(Bi_4O_6^+)C_2H_4$ (adduct b of Figure 8) by a strongly exoergic process (-32.7 kcal mol^{-1}). The resulting complex exhibits a radical nature with the unpaired electron being localized on the terminal carbon atom. Furthermore, it is important to emphasize that all attempts to locate a TS structure along the specified reaction coordinates failed in both constrained and unconstrained PES−TS optimization. This can be considered as an indication that the reaction might occur also due to very favorable kinetics. Since the complex $(Bi_4O_6^+)$-C_2H_4 (cf. Figure 8b) with the radical center has been identified in experiments as well, but as a reactive intermediate, we studied addition of O_2 to this complex following the idea that molecular oxygen will attack the organic substrate of the complex. In fact, it has been found (steps b and c) of Figure 8) that the addition of O_2 is a very exoergic process ($\Delta H°_{298} = -30.4$ kcal mol^{-1}) leading to superoxide species $(Bi_4O_6^+)C_2H_4O_2$ (cf. adduct c of Figure 8). Also in this case, a TS structure could not be located probably due (cf. see also accompanying paper[9]) to the high reactivity of radical species such as $(Bi_4O_6^+)C_2H_4$.

Stimulated by this result and by the experimental findings, we investigated the possibility that the radical reactions could proceed via addition of another ethene forming an C−C−O−O−C−C pattern attached to the cluster until dissociation of some species might occur. Accordingly, reaction of the superoxide species $(Bi_4O_6^+)C_2H_4O_2$ with an ethene gives rise to a exoergic process (steps c to d of Figure 8) with the energy gain of 7.1 kcal mol^{-1}, which is considerably smaller than those of the previous steps. Also the reaction leading to $(Bi_4O_6^+)$-$C_2H_4O_2C_2H_4$ is characterized by nearly zero energy barrier. Notice that the adduct d of Figure 8 closely resembles a peroxide species, with an extremely activated O−O bond (1.46 Å), which can be considered as a precursor for bond breaking producing

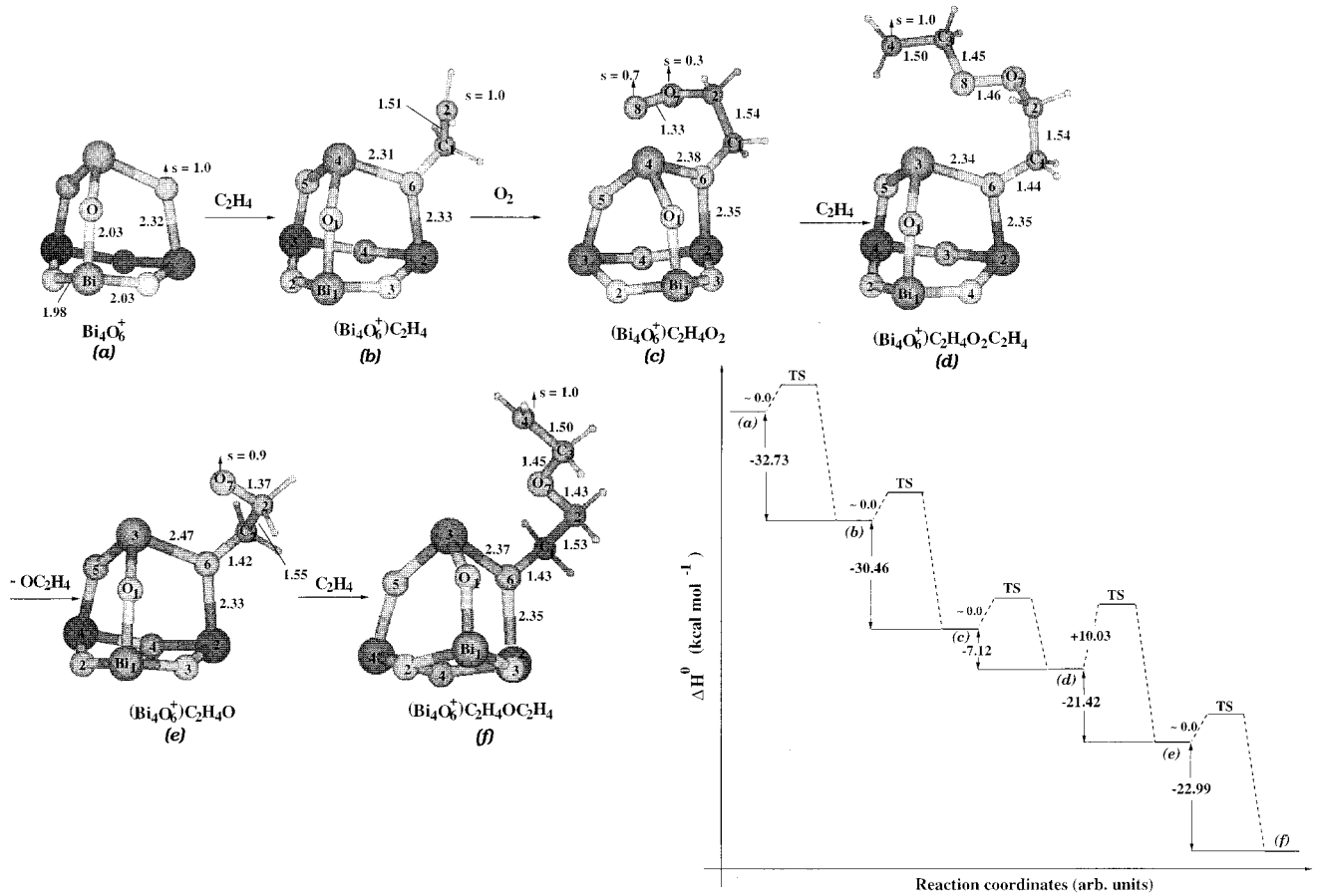

Figure 8. Structures and energetics of complexes with the $Bi_4O_6^+$ cluster obtained by adding molecular oxygen and ethene (b−d) and releasing oxirane (e), and adding ethene (*f*).

TABLE 6: Energies of the Most Stable Structures of $(Bi_4O_6^+)O_y(C_2H_4)_z$ ($y = 0-3$; $z = 1, 2$) Complexes

structures	E_{DFT} (au)	$H°_{DFT}$ (au)
$(Bi_4O_6^+)C_2H_4$ (b)[a]	−130.876 892	−130.789 983
$(Bi_4O_6^+)C_2H_4O_2$ (c)[a]	−162.748 185	−162.648 492
$(Bi_4O_6^+)C_2H_4O_2C_2H_4$ (d)[a]	−176.417 722	−176.261 679
$(Bi_4O_6^+)C_2H_4O$ (e)[a]	−146.843 400	−146.750 800
$(Bi_4O_6^+)C_2H_4OC_2H_4$ (f)[a]	−160.541 062	−160.389 285
$(Bi_4O_6^+)C_2H_4OC_2H_4O_2$ (k)[b]	−192.413 183	
$(Bi_4O_6^+)C_2H_4OC_2H_4O_2C_2H_4$ (l)[b]	−206.084 347	
THF[c]	−43.342 689	−43.221 853

[a] For geometries of clusters cf. Figure 8b−f. [b] Complexes involved in path V of Figure 9. [c] Tetrahydrofuran (path II of Figure 9).

oxirane. Indeed, such a dissociation occurs easily from an energetic point of view (the computed reaction energy is $\Delta H°_{298} = -21.4$ kcal mol^{-1}). Also the required activation energy is relatively small, since the TS structure has been located only at +10.0 kcal mol^{-1} above the reactants as shown in Figure 8 for step d to e: an oxirane molecule is released and a radical species of stoichiometry $(Bi_4O_6^+)C_2H_4O$ is formed (the TS structure is omitted in Figure 8). The latter species can, in principle, react following different paths: (i) to dissociate a second OC_2H_4 molecule and restore the $Bi_4O_6^+$ cluster, (ii) to react with molecular oxygen leading to an ozonide-like species, or (iii) to react further with an additional ethene molecule. Path (i) requires the dissociation of a bond between the C atom of the C_2H_4O group and an oxygen atom belonging to the cluster frame. For this process a reaction enthalpy $\Delta H°_{298} = +42.2$ kcal mol^{-1} is needed and an even higher reaction barrier might be present. Therefore it can be considered as an unfavorable reaction path. For the second path (ii) neither theoretical nor experimental evidence has been found. Finally path (iii) which corresponds to the steps e and f of Figure 8 is thermodynamically favorable by an extent of 23.0 kcal mol^{-1} and seems to occur in the absence of activation energy. This confirms all our theoretical findings for bimolecular reactions involving radical species. Notice that the adduct f of Figure 8 closely resembles a radical ether.

The above-discussed chain process certainly involves unusual chemical species which actually have been so far identified by quantum chemical calculation only. However, all these species have been detected experimentally and a particularly high reactive cross section for $Bi_4O_6^+$ due to reactive collisions has been observed (cf. accompanying paper[9]). Furthermore, in the presence of a mixture of ethene and molecular oxygen only a small quantity of $(Bi_4O_6^+)C_2H_4$ (adduct b of Figure 8) has been formed whereas other species have been identified with molecular masses corresponding to $(Bi_4O_6^+)C_2H_4O_2$ (adduct c) and $(Bi_4O_6^+)C_2H_4O_2C_2H_4$ (adduct d) as well as $(Bi_4O_6^+)C_2H_4O$ (adduct e) and $(Bi_4O_6^+)C_2H_4OC_2H_4$ (adduct f). Of course, the claim cannot be made that the reaction mechanism based on our theoretical investigation represents the only way that reactions can proceed. However, our mechanism seems to be realistic under the assumption that no more than one ethene molecule can be attached directly to $Bi_4O_6^+$. This has been confirmed by the fact that no experimental evidence has been obtained for the existence of species such as $C_2H_4(Bi_4O_6^+)C_2H_4$ and $O_2C_2H_4(Bi_4O_6^+)C_2H_4O_2$.

6. The Role of $Bi_4O_6^+$ in Catalytic Oxidation

The determined reactive properties of the $Bi_4O_6^+$ cluster described in previous sections will be used to design a complete thermodynamic cycle. As is well-known, oxidation processes

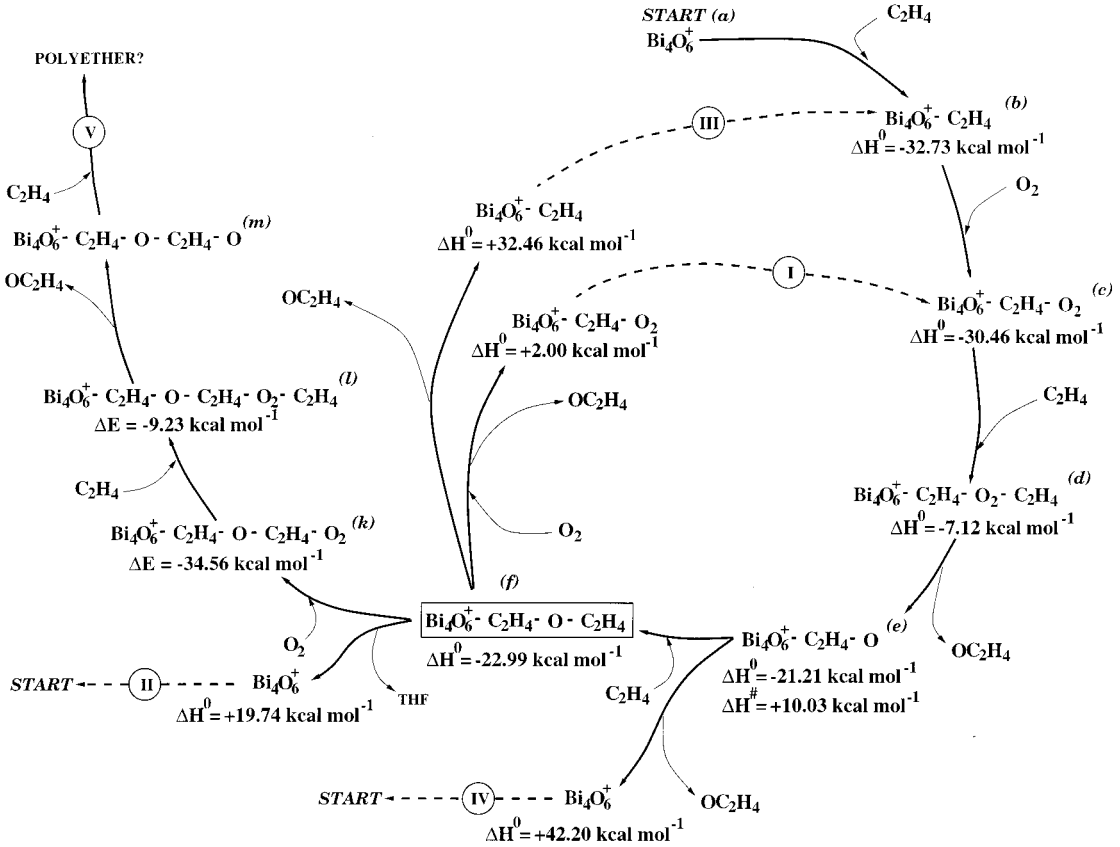

Figure 9. Thermodynamic cycle starting from $Bi_4O_6^+$ following Figure 8 (right side) (steps a−f) extended by formation of chain through C_2H_4O units by adding molecular oxygen and ethane (steps k−m).

involving heterogeneous catalysts usually occur via adsorption and activation of molecular oxygen. In the case of transition metal[28] homogeneous catalysts, the activation of O_2 usually requires that the metal is in a low oxidation state.[31] The chemistry of bismuth[31,32] is dominated by compounds (cf. Bi_2O_3) with the metal atoms in +3 formal oxidation state. Mainly due to relativistic effects, and inert pair effects of s electrons, compounds with the metal atoms in lower or higher oxidation states do exist only under very special conditions.[31] Therefore, forms such as $Bi_4O_6^+$ are expected to be particularly stable since the transfer of oxygen atoms to substrate would change the oxidation state of the metal. This observation has been considered as the key assumption in proposing our reaction mechanism which involves activation of molecular oxygen acting as primary oxidant and leaving the cluster intact.

A stable compound with stoichiometry $(Bi_4O_6^+)C_2H_4OC_2H_4$ has been identified experimentally and theoretically. A proposed reaction mechanism for the formation of these products involves reactions with C_2H_4, O_2, and $Bi_4O_6^+$ species, where the bismuth oxide plays a crucial role in the indirect activation of molecular oxygen leading to the formation of hydrocarbon peroxide species and oxidized ethene by exoergic processes (cf. Table 6).

The question can be raised whether a catalytic cycle can be designed based on the computed properties. The attempt has been made in Figure 9. The right part of the figure (steps a−f) summarizes our findings presented in Figure 8 and discussed in a previous section showing that $Bi_4O_6^+$ easily reacts with ethene and molecular oxygen to form stable adducts which can be considered as intermediates (species b−f) or products (OC_2H_4).

Here we wish to address the role of f and e adducts. Starting from adduct e, the cycle can be closed by following path IV of Figure 9 in which the adduct e would release an oxirane molecule to give back the $Bi_4O_6^+$ oxide, but this process is both thermodynamically and kinetically unfavorable since the reaction enthalpy amounts to +42.9 kcal mol^{-1}.

By considering adduct f, the paths II and III are also unlikely to occur due to endoergicity of +19.7 and +32.4 kcal mol^{-1}, respectively. Furthermore, notice that, in the case of path III, the cycle closes to intermediate b and not to the $Bi_4O_6^+$.

Path I is only slightly thermodynamically unfavorable, although from kinetics considerations this reaction is not likely to occur. The intermediate f is involved in a bimolecular reaction with O_2. Namely, oxirane molecule is released and the cycle closes to intermediate c, but the reaction mechanism would involve a first-order nucleophilic substitution reaction. Since the free molecular oxygen is not a very strong nucleophilic species and the involved carbon atom (cf. C_2 of Figure 8) has a small fraction of negative charge (from NAO charge analysis population), it is to be expected that the high activation barrier would prevent the reaction from taking place.

In Figure 9 we report also path V, which we consider to be the most favorable one. By adding an O_2 molecule to adduct f which retains radical properties as discussed in the previous section, adduct k can be formed due to a "chain mechanism", differing from adduct c by an additional OC_2H_4 "chain unit". The reaction enthalpy has been computed as −34.6 kcal mol^{-1}, and we have not been able to locate the TS structure similarly as in the previously energetically favorable cases (such as a−d). The similarity of adducts k and c suggested to us to investigate the possibility that a polyether chain supported on the $Bi_4O_6^+$ cluster can be formed. In fact, the peroxide species l differs from d also by an OC_2H_4 unit only. It is important to emphasize that the energetics of reaction path f−l compares well to the

one calculated for b−d of Figure 9, which means that the reaction along path V could be favorable. Furthermore, Figure 9 shows that once $Bi_4O_6^+$ species has been formed and has initiated the reaction giving rise to $Bi_4O_6^+$-C_2H_4−O−C_2H_4 (f), it plays a spectator role along path V since the chain reaction proceeds by elongation through the OC_2H_4 units.

Of course, species with high masses such as k, l, and m have not been detected experimentally since their masses are out of the range belonging to $Bi_4O_y^+$ ($y = 1-n$) series and overlap with the oxide cluster with stoichiometry $Bi_5O_y^+$ ($y = 1-n$). Furthermore, the experimental setup consists of a very short reaction channel (allowing for the limited number of reactive collisions) in which only a small fraction of ethene is present in comparison with molecular oxygen, reducing the probability for detection of these species. Nevertheless, our theoretical findings concerning the path V suggest that the mechanism involving OC_2H_4 chain units attached to $Bi_4O_6^+$ cluster might be an interesting process for future experimental investigations of the role of clusters as model systems for catalysis.

7. Conclusions

Our systematic study of structural and electronic properties of the $Bi_3O_y^+$ ($y = 3-6$) and $Bi_4O_y^+$ ($y = 6-8$) clusters as well as their interaction with ethene based on density functional approach gives rise to three important findings:

I. Transfer of oxygen atoms from the stable clusters such as $Bi_3O_4^+$ is an energetically unfavorable process due to the breaking of strong Bi−O bonds, but in the presence of O_2 these clusters can be activated and oxidation of ethene might become feasible.

II. The key role of $Bi_4O_6^+$ has been established, since it interacts easily with ethene giving rise to a complex with a radical center located at a carbon atom and allowing the molecular oxygen to form a "superoxide" unit which is ready to further react with other ethene to produce "peroxides", confirming the experimental findings of the accompanying paper.[9]

III. The formation of chain with reactive ($^\bullet OC_2H_4$) units attached to the $Bi_4O_6^+$ cluster allows for possible oligomer formation from the energetic point of view.

We can conclude that bismuth oxide clusters such as $Bi_4O_6^+$, retaining their identity, can play an important role in the presence of molecular oxygen for oxidation processes of alkenes.

Acknowledgment. This work has been supported by the Deutsche Forschungsgemeinschaft (SFB 450 Analysis and Control of Ultrafast Photoinduced Reactions). M.B. thanks the Università di Milano for partial support.

Supporting Information Available: Cartesian coordinates of the 18 most relevant computed molecular structures. This material is available free of charge via the Internet at http://pubs.acs.org.

References and Notes

(1) (a) Cheilliah, D.; Keulks, G. W. *J. Catal.* **1972**, *24*, 529. (b) Grasselli, R. K.; Burrington, D. J. *Adv. Catal.* **1981**, *30*, 133. (c) Centi, G.; Perathoner, S. *Appl. Catal., A* **1995,** *124*, 317.

(2) Taylor, S. H.; Hargreaves, J. S. J.; Hutchings, G. J.; Joyner, R. W. *Appl. Catal., A* **1995**, *126*, 287.

(3) (a) Snyder, T. P.; Hill, C. G. *J. Catal. Rev.-Sci. Eng.* **1989**, *31* (1&2), 43 and references therein. (b) Sachtler, W. M. H. *Catal. Rev.* **1970**, *4* (1), 27.

(4) Swift, E.; Bozik, J. E.; Ondrey, J. A. *J. Catal.* **1971**, *21*, 212.

(5) (a) Zhou, B.; Machej, T.; Ruiz, P.; Delmon, B. *J. Catal.* **1991**, *132*, 183. (b) Delmon, B. *Heterog. Chem. Rev.* **1994**, *1*, 219.

(6) (a) Kinne, M.; Heidenreich, A.; Rademann, K. *Angew. Chem., Int. Ed.* **1998**, *37*, 18. (b) Kinne, M.; Bernhardt, T. M.; Kaiser, B.; Rademann, K. *Int. J. Mass Ion. Processes* **1997**, 167/168, 161. (c) Kaiser, B.; Bernhardt, T. M.; Kinne, M.; Rademann K.; Heidenreich, A. *J. Chem. Phys.* **1999**, *110*, 3.

(7) France, M. R.; Buchanan, J. W.; Robinsons, J. C.; Pullins, S. H.; Tucker, J. L.; King, R. B.; Duncan, M. A. *J. Phys. Chem. A* **1997**, *101*, 6214.

(8) Kinne, M.; Bernhardt, T. M.; Kaiser, B.; Rademann, K. *Z. Phys. D* **1997,** *40*, 105.

(9) Fielicke, A.; Rademann, K. *J. Phys. Chem. A* **2000**, *104*, 6979.

(10) Becke, A. D. *J. Chem. Phys.* **1997**, *107*, 8554.

(11) Curtiss, L. A.; Raghavachari, K.; Trucks, G. W.; Pople, J. A. *J. Chem. Phys.* **1991**, *94*, 7221.

(12) Becke, A. D. *J. Chem. Phys.* **1993**, *98*, 5648.

(13) Hamprecht, F. A.; Cohen, A. J.; Tozer, D. J.; Handy, N. C. *J. Chem. Phys.* **1998**, *109*, 15.

(14) Bienati, M.; Adamo, C.; Barone, V. *Chem. Phys. Lett.* **1999**, *311*, 69.

(15) Stevens, W. J.; Krauss, M.; Basch, H.; Jasien, P. G. *Can. J. Chem.* **1992**, *70*, 612. Cundari, T. R.; Stevens, W. J. *J. Chem. Phys.* **1993**, *98*, 5555.

(16) Stevens, W. J.; Basch, H.; Krauss, M. *J. Chem. Phys.* **1984**, *81*, 6026.

(17) a) Huber, K. P.; Herzberg, G. *Molecular Spectra and Molecular Structure IV. Constants of Diatomic Molecules*; Van Nostrand Reinhold Co.: London, 1979. (b) Huheey, J. E.; Keiter, E. A.; Keiter, R. L. *Inorganic Chemistry: Principles of structure and reactivity*, 4th ed.; HarperCollins: New York, 1993. (c) Lide, D. R. *CRC Handbook of Chemistry and Physics*, 75th ed.; CRC Press: Boca Raton: FL, 1994.

(18) Schlegel, H. B. In *Modern Electronic Structure Theory*; Yarkony, D. R., Ed.; World Scientific Publishing: Singapore, 1994; Vol. 2, and references therein.

(19) Peng, C.; Ayala, P. Y.; Schlegel, H. B.; Frisch, M. J. *J. Comput. Chem.* **1996**, *17*, 49.

(20) (a) Peng, C.; Schlegel, H. B. *Isr. J. Chem.* **1993**, *33*, 449. (b) Peng, C.; Ayala, P. Y.; Schlegel, H. B.; Frisch, M. J. *J. Comput. Chem.* **1995**, *16*, 49.

(21) Frisch, M. J.; Trucks, G. W.; Schlegel, H. B.; Scuseria, G. E.; Robb, M. A.; Cheeseman, J. R.; Zakrzewski, V. G.; Montgomery, J. A., Jr.; Stratmann, R. E.; Burant, J. C.; Dapprich, S.; Millam, J. M.; Daniels, A. D.; Kudin, K. N.; Strain, M. C.; Farkas, O.; Tomasi, J.; Barone, V.; Cossi, M.; Cammi, R.; Mennucci, B.; Pomelli, C.; Adamo, C.; Clifford, S.; Ochterski, J.; Petersson, G. A.; Ayala, P. Y.; Cui, Q.; Morokuma, K.; Malick, D. K.; Rabuck, A. D.; Raghavachari, K.; Foresman, J. B.; Cioslowski, J.; Ortiz, J. V.; Stefanov, B. B.; Liu, G.; Liashenko, A.; Piskorz, P.; Komaromi, I.; Gomperts, R.; Martin, R. L.; Fox, D. J.; Keith, T.; Al-Laham, M. A.; Peng, C. Y.; Nanayakkara, A.; Gonzalez, C.; Challacombe, M.; Gill, P. M. W.; Johnson, B.; Chen, W.; Wong, M. W.; Andres, J. L.; Gonzalez, C.; Head-Gordon, M.; Replogle, E. S.; Pople, J. A. *Gaussian 98*, Revision A.5; Gaussian, Inc.: Pittsburgh, PA, 1998.

(22) (a) Barrow, G. M. *Physical Chemistry*, 4th ed.; McGraw-Hill: New York, 1988. (b) Reif, F. *Fundamentals of Statistical and Thermal Physics*; McGraw-Hill: International Edition: New York, 1985.

(23) Truhlar, D. G.; Garrett, B. C.; Klippenstein, S. J. *J. Phys. Chem.* **1996**, *100*, 12771 and references therein.

(24) Baboul, A. G.; Schlegel, H. B. *J. Chem. Phys.* **1997**, *107*, 9413.

(25) Reed, A. E.; Curtiss, L. A.; Weinhold, F. *Chem. Rev.* **1988**, *88*, 899 and references therein.

(26) Mulliken, R. *J. Chem. Phys.* **1955**, *23*, 1833.

(27) Luthi, H. P.; Ammeter, J. H.; Almlöf, J.; Faegri, K. *J. Chem. Phys.* **1982**, *77*, 2002.

(28) (a) Fantucci, P.; Lolli, S. *J. Mol. Catal.* **1993**, *82*, 131 and references therein. (b) Fantucci, P.; Lolli, S.; Pizzotti, M. *Inorg. Chem.* **1994**, *33*, (13), 2779.

(29) Doornkamp, C. *The activation of oxygen by metal oxide catalysts*; Ponsen & Looijen bv: Wageningen, 1998.

(30) We investigated the production of oxirane as first oxidized intermediate in the oxidation of ethene. This relatively stable species could however further transform to other more stable oxides (e.g., acetaldehyde). Since the present study addresses the energetics of oxygen transfer reactions involving bismuth oxide clusters, we focused on oxirane as product.

(31) Cotton, F. A.; Wilkinson, G. *Advanced Inorganic Chemistry*; John Wiley & Son: New York, 1984.

(32) Huheey, J. E.; Keiter, E. A.; Keiter, R. L. *Inorganic Chemistry: Principles of Structure and Reactivity*, 4th ed.; HarperCollins: New York, 1993.